

Magnetic ordering in pyrochlore $\text{Ho}_2\text{Mn}_2\text{O}_7$

N. P. Raju and J. E. Greedan

Brockhouse Institute for Materials Research, McMaster University, Hamilton, Ontario L8S 4M1, Canada

J. S. Pedersen

Department of Solid State Physics, Risø National Laboratory, DK-4000 Roskilde, Denmark

Ch. Simon and A. Maignan

Laboratoire CRISMAT, CNRS URA 1318, ISMRa, Université de Caen, Bd du Maréchal Juin, 14050 Caen Cédex, France

A. M. Niraimathi and E. Gmelin

Max-Planck-Institut für Festkörperforschung, Heisenbergstrasse 1, 70569 Stuttgart, Germany

M. A. Subramanian

Central Research and Development, E.I. DuPont de Nemours and Co., Wilmington, Delaware 19880-0328

The magnetic susceptibility of $\text{Ho}_2\text{Mn}_2\text{O}_7$ with a spontaneous rise below about 40 K and a paramagnetic Curie temperature of +39 K suggests a ferromagnetic ordering. Indeed neutron diffraction profiles show strongly enhanced Bragg peaks with a temperature dependence which indicates an apparent $T_c \approx 35$ K. Nonetheless, the magnetic diffraction pattern is not consistent with a collinear ferro or ferrimagnetic ordering of the Ho^{3+} and Mn^{4+} sublattices. Furthermore, specific heat and small angle neutron scattering (SANS) show features which are also incompatible with conventional long-range order. © 1996 American Institute of Physics. [S0021-8979(96)24008-9]

I. INTRODUCTION

Two necessary but not sufficient conditions for the occurrence of spin-glass-like ordering in a given material are site disorder and magnetic frustration.¹ Recently, some pyrochlore structure materials have been studied extensively as they seem to exhibit spin-glass-like ordering based on magnetic frustration alone, having apparently negligible site disorder.²⁻⁸ The pyrochlore compounds $\text{R}_2\text{M}_2\text{O}_7$ (R^{3+} =rare earth; M^{4+} =transition metal) crystallize in the face-centered-cubic structure with the space group $\text{Fd}3m$.⁹ Each of the metal atoms in these compounds forms a three-dimensional network of corner-sharing tetrahedra. Such a topology leads to a very high degree of magnetic frustration if the nearest neighbor interactions are antiferromagnetic.¹⁰

The series of pyrochlores $\text{R}_2\text{Mn}_2\text{O}_7$ ($\text{R}=\text{Dy}-\text{Lu}$, or Y) have been reported to show ferromagnetic ordering based upon the observation of positive θ_p values and spontaneous magnetization.³ Further studies of neutron scattering and heat capacity provided no evidence for long-range magnetic ordering in $\text{Y}_2\text{Mn}_2\text{O}_7$.⁴ Small angle neutron scattering (SANS) studies indicated the presence of ferromagnetic clusters of finite size in the temperature range 13–20 K.⁶ A variety of studies on a related series of compounds $\text{R}_2\text{Mn}_2\text{O}_7$ ($\text{R}=\text{Sm}$, Gd , Tb , or Y) demonstrate the presence of spin-glass-like ordering.^{5,7,8} In contrast recent studies of magnetic and electrical along with SANS data on $\text{Tl}_2\text{Mn}_2\text{O}_7$ and $\text{In}_2\text{Mn}_2\text{O}_7$ are consistent with the long-range ferromagnetic ordering below about 120 K in both materials.¹¹

$\text{Ho}_2\text{Mn}_2\text{O}_7$ has been reported to show spontaneous magnetization below about 40 K with a paramagnetic Curie temperature, θ_p , of +33 K.³ To understand the nature of this magnetic ordering, a variety of studies, ac and dc magnetic susceptibilities, specific heat, SANS and powder neutron diffraction were performed and the results are discussed in Sec. III.

II. EXPERIMENT

The polycrystalline powder sample used in the present measurements is the same as that described in Ref. 3. Ac susceptibility, χ' , was determined as function of temperature using a Lake Shore 7000 Susceptometer. Dc susceptibility and magnetization were measured with the help of a SQUID magnetometer (Quantum Design, San Diego). The specific heat of the sample, in the form of powder, was measured in the temperature range 2–90 K using a fully automated quasi-adiabatic calorimeter equipped with a Ge thermometer. The SANS experiments were performed at the instrument at the DR3 reactor at Risø National Laboratory. The powder neutron diffraction data, at different temperatures were obtained at the McMaster Nuclear Reactor with 1.3913 Å neutrons.

III. RESULTS AND DISCUSSION

Figure 1 shows the temperature dependence of the real part of the ac susceptibility, χ' , of $\text{Ho}_2\text{Mn}_2\text{O}_7$ at 10 G at different frequencies χ' increases rapidly below about 40 K

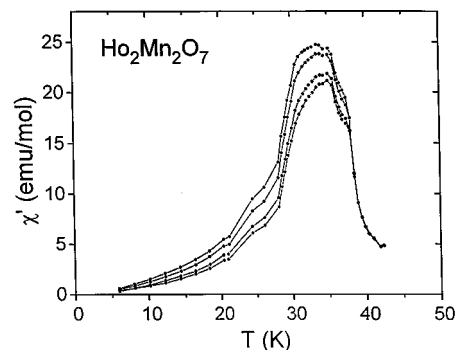


FIG. 1. ac susceptibility, χ' , of $\text{Ho}_2\text{Mn}_2\text{O}_7$ at four different frequencies, from top to bottom: (8, 33, 143, and 222 Hz).

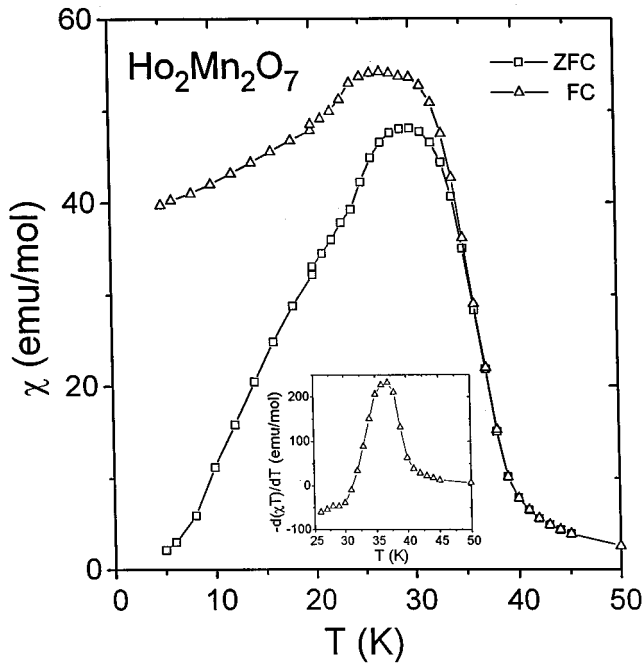


FIG. 2. Zero field cooled (ZFC) and field cooled (FC) dc susceptibility of $\text{Ho}_2\text{Mn}_2\text{O}_7$ measured at 100 G. The inset shows the negative temperature derivative of the product of the FC susceptibility and temperature.

and frequency dependent behavior is seen below 38.0 K with a broad maxima around 33 K. The dc susceptibility, measured at 100 G, is plotted against temperature in Fig. 2. It can be seen that a spontaneous magnetization develops below about 40 K and deviations occur between zfc and fc susceptibilities below 35 K which is expected for a spin-glass transition. A plot of $-d(\chi T)/dT$ against T is generally useful to determine the transition temperature more accurately from the dc susceptibility data. Such a plot given in the inset of Fig. 2 indicates a T_c of 37.1 ± 1.0 K. The magnetization as a function of applied field was measured at 5.0 K. Saturation occurs only above 1.5 T with a value of $12.3 \mu_B/\text{Ho}_2\text{Mn}_2\text{O}_7$ at 5.0 T. In $\text{Y}_2\text{Mn}_2\text{O}_7$ a magnetic moment of $2.3 \mu_B/\text{Mn}$ at 4.0 T was reported.⁴ Assuming the same Mn^{4+} sublattice contribution in $\text{Ho}_2\text{Mn}_2\text{O}_7$ leaves a saturation moment of $3.9 \mu_B/\text{Ho}^{3+}$ which is very small compared with an expected value of $gJ = 10.0 \mu_B$ per Ho^{3+} free ion ($g = 1.25$ and $J = 8$

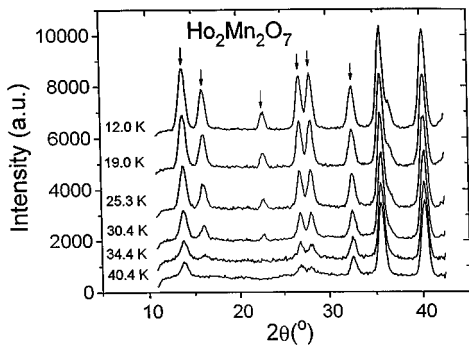


FIG. 3. Powder neutron diffraction profiles at different temperatures for $\text{Ho}_2\text{Mn}_2\text{O}_7$. The base line intensities for different temperatures are shifted arbitrarily for the clarity of the plots.

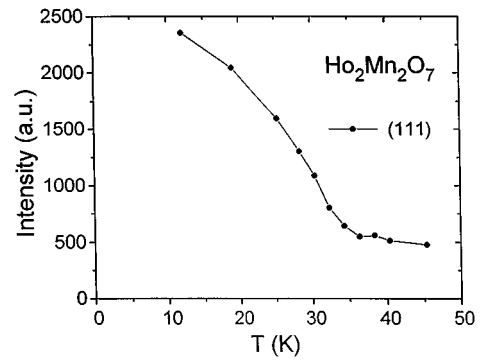


FIG. 4. The intensity of the Bragg reflection (111) against temperature.

for Ho^{3+} with a ground state of 2I_8). The significant reduction in Ho^{3+} moment from the expected value suggests the existence of strong crystal field effects. This is consistent with the specific heat data discussed later.

The powder neutron diffraction profiles at different temperatures are plotted in Fig. 3. First, note that the intensity of each nuclear Bragg peak, indicated by the arrows, is enhanced as the temperature is decreased and that there is no apparent change in the peak width. Further the temperature dependence of the intensity of the (111) reflection at 13.85°, as shown in Fig. 4, is consistent with the susceptibility data in suggesting a T_c of about 36 K. The observed magnetic diffraction pattern is not consistent with a collinear ferro or ferrimagnetic structure as found for $\text{Nd}_2\text{Mo}_2\text{O}_7$ or $\text{Yb}_2\text{V}_2\text{O}_7$

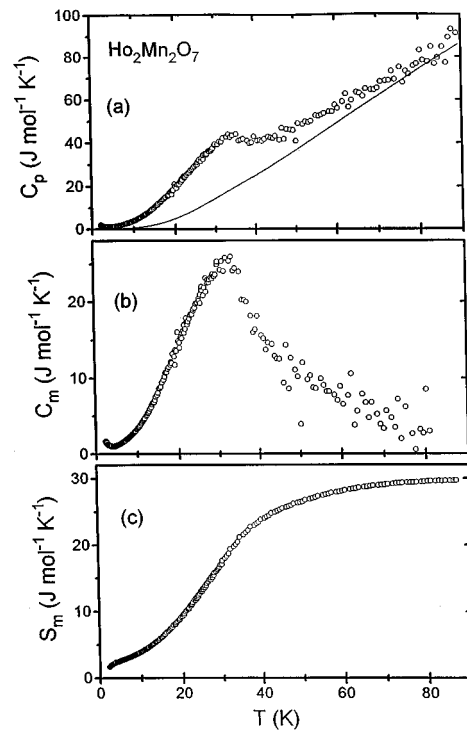


FIG. 5. (a) Measured specific heat, C_p , of $\text{Ho}_2\text{Mn}_2\text{O}_7$. The continuous line represents the estimated lattice specific heat, C_l . (b) Magnetic specific heat, C_m , obtained by subtracting the C_l from the C_p . (c) Magnetic entropy, S_m , vs temperature.

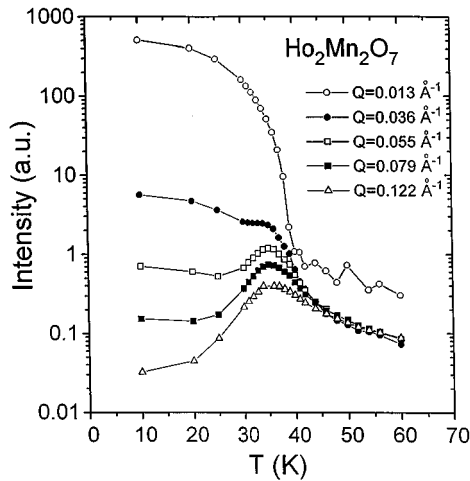


FIG. 6. Small-angle neutron-scattering intensity (in arbitrary units) as a function of temperature at different wave vectors for $\text{Ho}_2\text{Mn}_2\text{O}_7$.

and no solution has yet been found.^{5,12} From the resolution of our neutron diffraction data we determine a lower limit for the spin correlation length of $\sim 115 \text{ \AA}$.

The measured specific heat, C_p , of $\text{Ho}_2\text{Mn}_2\text{O}_7$ in Fig. 5(a) displays an anomaly at about 35 K. The C_p of insulating $\text{Ho}_2\text{Mn}_2\text{O}_7$ consists of contributions from the lattice specific heat, C_l , and the magnetic specific heat, C_m . The C_l of $\text{Ho}_2\text{Mn}_2\text{O}_7$, represented by continuous line in Fig. 5(a), was evaluated to separate the contribution of C_m . The details of this procedure can be found in Ref. 7. The magnetic specific heat, in Fig. 5(b), shows a broad maximum around 33 K. The absence of a sharp λ -type anomaly and the presence of C_m to temperatures much above the apparent T_c suggests the absence of a conventional long-range magnetic ordering and the presence of short-range correlations. At temperatures below about 4 K there is an up turn in C_m . The magnetic entropy, S_m , involved in the magnetic anomaly is determined as a function of temperature by numerically integrating C_m/T (C_m/T behavior is extrapolated below 2 K). A plot of the magnetic entropy, S_m , versus temperature is displayed in Fig. 5(c). It can be seen that S_m reaches a value of $30 \text{ J mol}^{-1} \text{ K}^{-1}$ at 90 K which is far less than the expected magnetic entropy for $\text{Ho}_2\text{Mn}_2\text{O}_7$ with $J=8$ for Ho^{3+} and $S=3/2$ for Mn^{4+} , $2R \ln(2J+1) + 2R \ln(2S+1) = 70.2 \text{ J mol}^{-1} \text{ K}^{-1}$. This corroborates the reduced saturation moment of Ho^{3+} described above.

Figure 6 displays the temperature dependence of the scattered neutron intensity at different wave vectors, Q . For the highest wave vector (i.e., $Q=0.122 \text{ \AA}^{-1}$), the SANS intensity shows a broad maximum centering about 36 K, which is close to the T_c observed in the previously described experiments, and decreases with the temperature below the T_c . As the Q is reduced down to 0.055 \AA^{-1} , the broad maximum

and persists but the intensity rises towards the lower temperatures. With a further decrease in the Q , the intensity does not exhibit any peak but a plateau below 36 K and starts increasing below 30 K. For the lowest Q of 0.013 \AA^{-1} , the intensity increases sharply below 40 K and continues to increase with the decrease in the temperature. For a long-range ordered material, the SANS intensity observed at low Q as a function of the temperature shows a pronounced cusp at the T_c with a rapid fall off in the intensity both above and below the T_c . The SANS intensity of $\text{Ho}_2\text{Mn}_2\text{O}_7$, at the low Q of 0.013 \AA^{-1} , does not show any cusp at the T_c providing evidence for the absence of long-range magnetic ordering. It is of interest here to mention the SANS intensities of $\text{Tl}_2\text{Mn}_2\text{O}_7$ and $\text{Y}_2\text{Mn}_2\text{O}_7$ against temperature.¹¹ In $\text{Tl}_2\text{Mn}_2\text{O}_7$, the SANS intensity shows a sharp peak at the transition temperature indicating a long-range ordering and consistent with the other experimental evidence. However, in $\text{Y}_2\text{Mn}_2\text{O}_7$ where long-range order is absent, the SANS intensity rises sharply below the T_c . A detailed analysis of SANS data for $\text{Y}_2\text{Mn}_2\text{O}_7$, $\text{Ho}_2\text{Mn}_2\text{O}_7$, and $\text{Yb}_2\text{Mn}_2\text{O}_7$, to be published elsewhere, gives evidence for correlation lengths of the order of 500 \AA and greater associated with a random field scattering. It is thus likely that the apparently complex ordering seen in $\text{Ho}_2\text{Mn}_2\text{O}_7$ is not truly long range and thus it is possible to reconcile the neutron diffraction and heat capacity results.

ACKNOWLEDGMENTS

We thank Professor C. V. Stager for the use of the SQUID magnetometer and McMaster University for direct support of the McMaster Nuclear Reactor. The Natural Science and Engineering Research Council of Canada has provided financial support.

- ¹J. A. Mydosh, *Spin Glasses: An Experimental Introduction* (Taylor & Francis, London, 1993), p. 3.
- ²J. E. Greedan, M. Sato, X. Yan, and F. S. Razavi, *Solid State Commun.* **59**, 895 (1986).
- ³M. A. Subramanian, C. C. Torardi, D. C. Johnson, J. Panetier, and A. W. Sleight, *J. Solid State Chem.* **72**, 24 (1988).
- ⁴J. N. Reimers, J. E. Greedan, R. K. Kremer, E. Gmelin, and M. A. Subramanian, *Phys. Rev. B* **43**, 3387 (1991).
- ⁵J. E. Greedan, J. N. Reimers, C. V. Stager, and S. L. Penny, *Phys. Rev. B* **43**, 5682 (1991).
- ⁶J. E. Greedan, J. Avelar, and M. A. Subramanian, *Solid State Commun.* **82**, 797 (1992).
- ⁷N. P. Raju, E. Gmelin, and R. K. Kremer, *Phys. Rev. B* **46**, 5405 (1992).
- ⁸B. D. Gaulin, J. N. Reimers, T. E. Mason, J. E. Greedan, and Z. Tun, *Phys. Rev. Lett.* **69**, 3244 (1992).
- ⁹M. A. Subramanian, G. Aravamudan, and G. V. Subba Rao, *Mater. Res. Bull.* **15**, 1401 (1980).
- ¹⁰P. W. Anderson, *Phys. Rev.* **102**, 1008 (1956); R. Liebmann, *Statistical Mechanics of Periodic Frustrated Ising Systems* (Springer, Berlin, 1986), p. 117; J. N. Reimers, A. J. Berlinsky, and A. C. Shi, *Phys. Rev. B* **43**, 865 (1991).
- ¹¹N. P. Raju, J. E. Greedan, and M. A. Subramanian, *Phys. Rev. B* **49**, 1086 (1994).
- ¹²L. Soderholm, C. V. Stager, and J. E. Greedan, *J. Solid State Chem.* **43**, 175 (1982); G. V. Bazuev, O. V. Makarova, and G. P. Shveikin, *Russ. J. Inorg. Chem.* **28**, 1088 (1983).